COSTOVERTEBRAL JOINT BEHAVIOUR DURING FRONTAL LOADING OF THE THORACIC CAGE

M. Eckert[1,2], M. Fayet[1], L.Cheze[3], R. Bouquet[2], E. Voïglio[4], J.P Verriest[2]
[1] LMSo, I.N.S.A (Institut National des Sciences Appliquées) Lyon, France
[2] LBMC, I.N.R.E.T.S (Institut National de Recherche sur les Transports et leur Sécurité) Bron, France
[3] Laboratoire MECAL, Université Claude Bernard, Lyon, France
[4] Laboratoire d'anatomie de la faculté de médecine de Lyon-Nord, Université Claude Bernard, Lyon, France

ABSTRACT

The objective is to experimentally characterize the costovertebral articulations when the bony structure of a thoracic cage is submitted to a compressive load on the sternum. Two tests have been performed in order to document the kinematics of these joints and to determine the role of the intercostal muscles on the stability of the thoracic cage. The tests also aim at determining the global deformation of the thoracic cage. The results will permit to improve a finite element model of the thoracic cage.

KEY WORDS

Biomechanics, Joints, Kinematics, Thorax , Finite Element Models

IN THE 70's appeared the first finite element models of the thorax (Reddi, 1977; Roberts, 1979; Sundaram, 1977). At present, they are more and more elaborated for the purpose of simulation of the mechanical behaviour of the thorax when it is submitted to an impact and for the prediction of resulting injuries (Song, 1998; Allain, 1998). These models include bony elements such as ribs, sternum and vertebrae, as well as some muscles and internal organs.

Due to lack of data describing the mechanical properties of the costovertebral joints, the connection between the ribs and the vertebrae is not yet properly represented in current models. Ribs and vertebrae are rigidly fixed to each other, leading to unrealistic loading of the ribs. The aim of this study is to collect data on the relative contribution of constitutive elements of the thoracic cage in order to improve an existing finite element model of this body segment. In particular, it was attempted to determine if the hypothesis of the existence of a fixed axis of rotation between ribs and vertebrae, described by Kapandji in breathing movements (Kapandji, 1994), is valid or not in this loading context. Another objective was to characterize the influence of intercostal muscles on the overall behaviour of the entire rib cage when a compression force is applied onto the sternum.

There are two articular surfaces in costovertebral joints : the articulation between the head of the rib and its two corresponding vertebrae (costovertebral articulation) and the articulation between the costal tuberosity and the transverse apophysis of the lower vertebra (costotransverse articulation) (see Fig. 1). According to Kapandji, during breathing movements, the ribs rotate relatively to the vertebrae thanks to these articulations. The axis of this rotation movement passes through the centres of the costovertebral and costotransverse articulations (see Fig. 2). The displacement of the ribs is due to the action of the intercostal muscles (see Fig. 3).

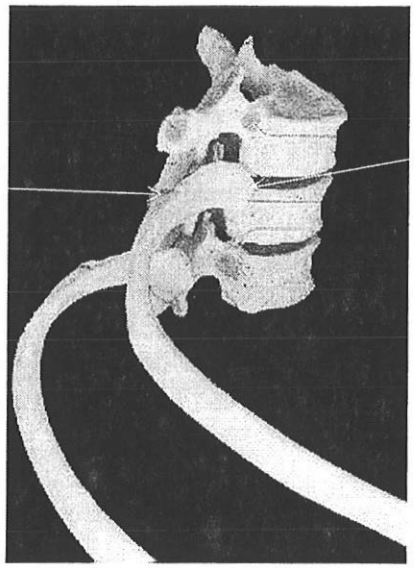

Fig. 1 - Costovertebral articulation (Rohen, 1999)

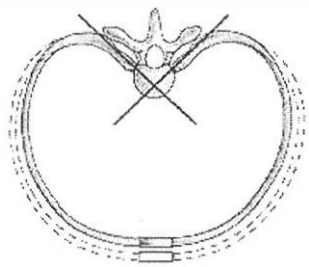

Fig. 2 - Movements of ribs relative to vertebrae (Rohen, 1999)

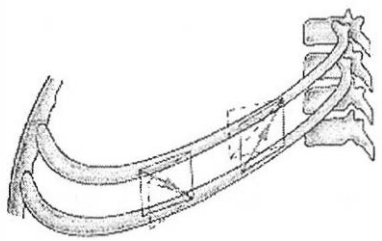

Fig 3 - Action of Intercostal Muscles (Rohen, 1999)

When an external force is applied to the sternum, such as those applied during a crash, the entire rib cage sustains a compression. The overall behaviour of the thorax has been described in models (Allain, 1998; Song, 1998) but the relative movement of the components is not known. What is the movement between ribs and vertebrae in this case, is there a fixed axis of rotation as stated before and what is the influence of the intercostal muscles on the overall behaviour, are the questions addressed by the experimental work reported here. In this first step, this study has been limited to the quasi-static case.

MATERIAL AND METHODS

EXPERIMENTAL SET-UP

Two tests have been performed on isolated thoracic segments. Experiments were conducted on unembalmed Post Mortem Human Subjects (PMHS) provided by the Faculty of Medicine of the University of Lyon. Subjects selected were free of any pathology of the spinal column. The thoracic cage was isolated and all the viscerae were removed. The vertebral column was sectioned at C7 and L1 levels. Skin, clavicle and scapula were taken away. The ligaments and intercostal muscles were preserved.

The vertebrae spinous processes were embedded in plaster in a rig, leaving the costovertebral joint free to move. So, the vertebrae remained fixed during experimentation.

The third, fifth and seventh left ribs have been equipped each with three triplets of markers covered with reflective paper (see Fig. 4). The first triplet is located near the chondro-costal junction, the second one approximately in the mid part of the rib and the third one near the costovertebral joint.

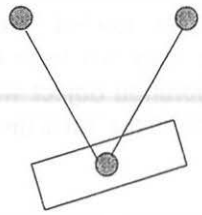

Fig. 4 - Triplet of reflective markers

Each triplet is composed of two small stainless steel rods (100 mm or 50 mm long and 2 mm diameter) terminated each by a 7 mm sphere and connected together by a common third sphere rigidly fixed on a 30*15 mm Plexiglas® plate (for the first and third triplets, the rods are 100 mm long and for the second triplet, they are 50 mm long). This plate was attached to the rib by means of mastic and nylon clamp collar. The triplet provides a local coordinate system for the rib area concerned.

The thoracic cage thus equipped has been placed under a loading machine (DELTALAB®) in order to apply quasi-static compressions on the sternum (see Fig. 5).

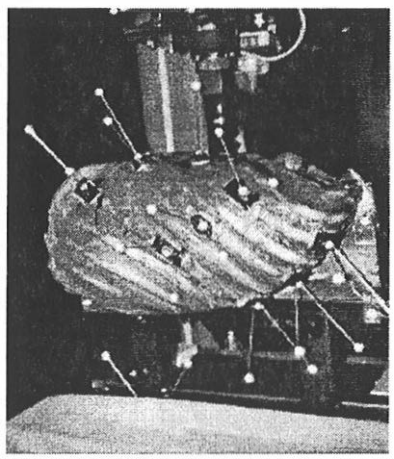

Fig. 5 - Thoracic cage equipped with triplets horizontally placed under the loading machine

DATA ACQUISITION

The displacement of the markers was recorded by a motion analysis system composed of four cameras (3D Vision® (N.T.C, 1994)) (see Fig. 6). Proper lighting was provided for each camera in order to obtain a high contrast of the retroreflective material covering the markers. Before the tests, a calibration phase was conducted with a known dimension (200*200*400 mm) calibration object including 12 markers, thus providing a global reference frame for the measurements.

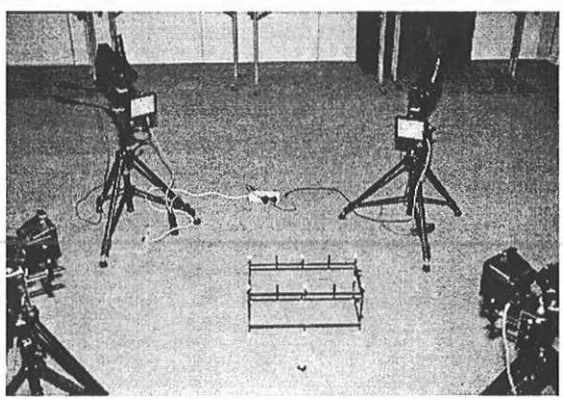

Fig. 6 - Motion Analysis system (3D Vision®) with the calibration object

The 3D marker displacements were reconstructed thanks to the software provided with the motion analysis system. The overall system accuracy has been evaluated by measuring the known distance between two markers fixed on a the calibration object which was submitted to a rotation movement. The maximum deviation obtained between the measured distance and the real distance is around 1 mm.

TEST PROTOCOL

A compression force was progressively applied on the sternum at three different levels with a rate of 8 mm/mn. The first application point was located in the middle of the sternum, the second one in the lower part of the sternum and the third one in the upper part of the sternum. The compression was limited to 40 mm for each case, such that there was no chance of lesion of the thoracic cage. After each compression, the cage was allowed to recover its original shape. After the first three tests, the intercostal muscles were taken away and a last compression force was applied at the middle of the sternum until either a sternum or a rib fracture occurred. For all tests, the compression force and displacement of the application point on the sternum were continuously measured by appropriate sensors.

REFERENCE FRAMES

After compressions, a vertebral anatomical reference frame was determined for the third, fifth and seventh vertebrae (see Fig. 7). The $\vec{Z}$ axis is defined as a line joining the two centres of the vertebral plateaux. Vector $\vec{U}$ joins the bases of the two pedicles. Vector $\vec{X}$ results from the vectorial product of $\vec{U}$ and $\vec{Z}$ and normalization. Vector $\vec{Y}$ is the vectorial product of $\vec{Z}$ and $\vec{X}$.

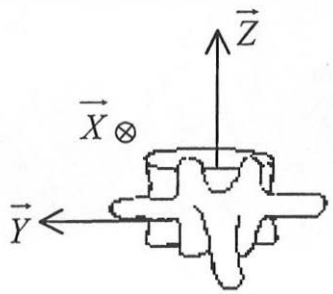

Fig. 7 - Anatomical reference frame of a vertebra

The position of the centres of vertebral plateaux and the basis of the pedicles are determined as follows, after the termination of the compressions. The first step is to cut off the ribs and to insert three Phillips screws® in each of the third, fifth and seventh vertebral bodies which provide 3 points to define a vertebral technical reference frame (see Fig. 8). The screws are inserted in order to have the largest possible distance between them. Their coordinates are determined with a 3D measuring arm (Faro®, 1997). The position and orientation of this vertebral technical reference frame with respect to the reference frame attached to the rig was then calculated.

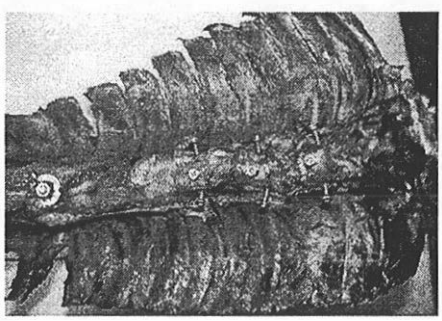

Fig. 8 - View of the inner face of the posterior part of the rib cage showing the screws inserted in the third, fifth and seventh vertebral bodies

Then, the third, the fifth and the seventh vertebrae were extracted and the position of the anatomical reference points (the two vertebral plateaux centres and the basis of the two pedicles) of each vertebrae were measured with respect to the technical frame based on the screws. Then, the transformation matrix between technical and anatomical frames could be calculated.

All the results presented are expressed in this anatomical reference frame for each vertebrae.

ROTATION AXIS DETERMINATION

To analyse the kinematics of the costovertebral articulation, every 5 mm of compression, the rotation axis for the movement of the third triplet (located near the costovertebral articulation) with respect to the spine was calculated. This calculation was performed for each of the three ribs 3, 5 and 7, with the method of Rodrigues (Rodrigues, 1840) (see ANNEX). Since the amplitude of the markers movement is very small, the measurement noise leads to a large scatter of the calculated axes. In order to reduce this noise, the solidification method proposed by Chèze and al. (Chèze, 1995) has been applied to the 3D coordinates of the markers. Moreover, since the displacement are continuously recorded at 25 frames per second and, provided that the rate of compression is 8 mm/mn, during 25 frames, the displacement of the application point of the compressive force is 0.13 mm. So, the displacement of the triplets could be assumed negligible for this period of time. Thus, it was averaged on 25 pictures at each step of compression. These techniques decrease noise in the 3D coordinates of the markers. Then, the method of Rodrigues is applied in order to determine the axis of rotation at the different steps.

A compression step was chosen for the determination of the rotation axis on the basis of a numerical simulation. This numerical simulation consisted in calculating the theoretical movement of points attached to a frame rotating around a perfectly known axis. The geometric arrangement of the points was analogous to that of the markers in the real experiment. A random noise with same amplitude of real measurement noise has been added to the coordinates of the points. The axis of rotation of the points was determined with the method of O. Rodrigues. The results of the simulation showed that the angle of rotation of the points must at least have a value of 3 degrees in order to expect an angular deviation less than 10 degrees between the calculated axis and the theoretical axis. Thus, in the results of our experiments, the axis of rotation for the first steps (when the angle of rotation is less then 3 degrees) will not be taken into account.

RESULTS

LOAD-DEFLECTION CHARACTERISTICS

The load-deflection curves obtained for the different compressions are presented on figures 9 to 12. The subject was a 76 years old male.

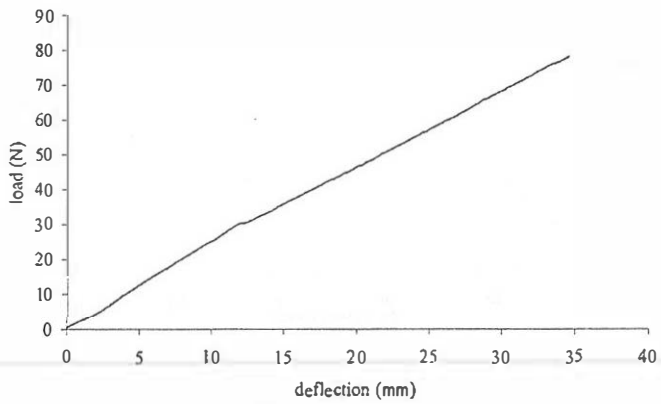

Fig. 9 - Load-deflection curve of the thoracic cage for the first compression (middle of the sternum) The viscerae have been removed but intercostal muscles are present.

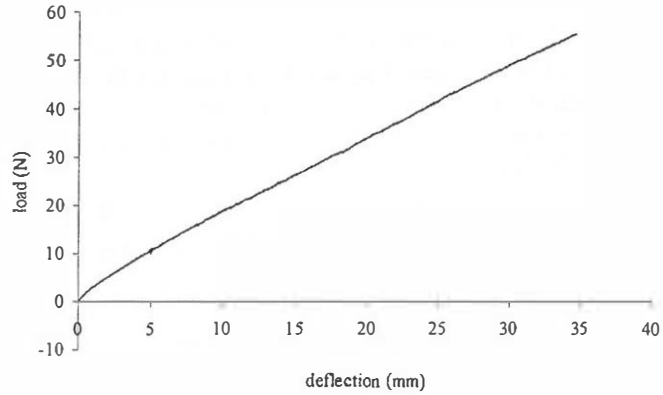

Fig. 10 - Load-deflection curve for the second compression (lower part of the sternum)

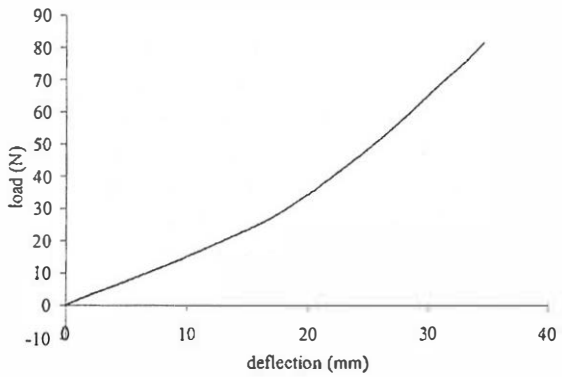

Fig. 11 - Load-deflection curve for the third compression (upper part of the sternum)

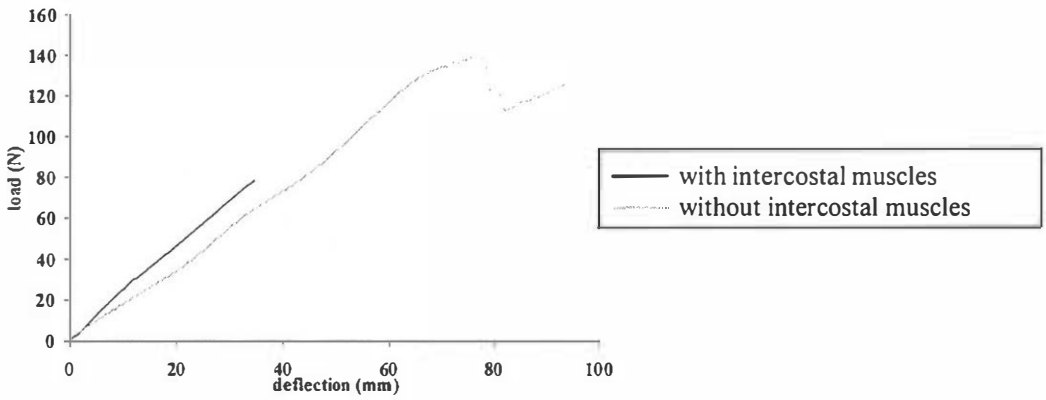

Fig. 12 - Load-deflection curves for the compression at the middle of the sternum with intercostal muscles and after their removal

The second subject was a 47 years old male. The load-deflection curve for the compression at the middle of the sternum is shown on figure 13.

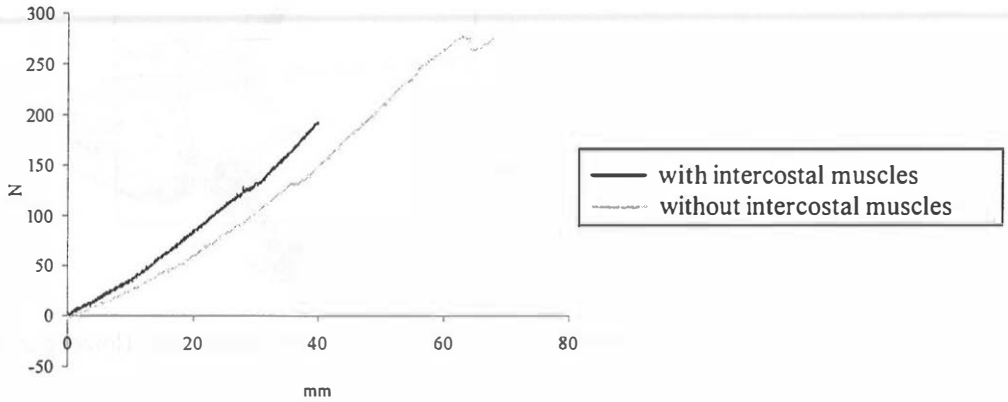

Fig. 13 - Load-deflection curve for a compression in the middle of the sternum

The global load-deflection curves are almost linear until a fracture occurs except for the third compression test (in the upper part of the sternum). The overall stiffness of the thoracic cage is much larger for the younger subject and is decreased when intercostal muscles are taken away (see Table 1). The first fracture which occurred was a fracture of the sternum for both subjects.

Subject age	47	76
Mid sternum with muscle	4000 N/m	2400 N/m
Mid sternum without muscles	3300 N/m	1900 N/m

Table 1 - Average global stiffness (N/m) of the isolated rib cage with and without intercostal muscles.

Subject age	47	76
Depth of the thorax :		
- under sternal depth	180 mm	285 mm
- axillary depth	160 mm	235 mm
Width of the thorax :		
- under sternal width	305 mm	195 mm
- axillary width	265 mm	158 mm

Table 2 -- Antropometry of the subjects

RIB ROTATION AXIS WITH RESPECT TO VERTEBRA

The successive axes of rotation of the 5th rib with respect to the 5th vertebra calculated for the different sternum compression tests for the 76 years old subject are presented on figures 14 to 21. These axes were calculated for compression steps producing at least 3 degrees of rotation of the rib.

For figures 14 to 21 the scale is in millimetres and the origin of the axes lies in the middle of the vertebral body.

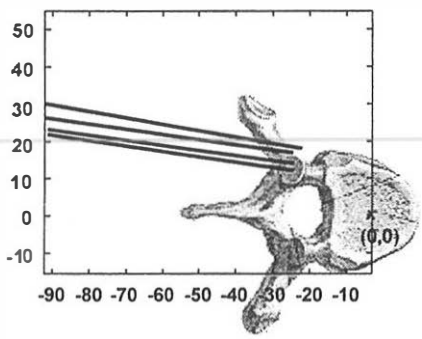

Fig. 14 - Axes of rotation during the first compression (middle of the sternum) (subject aged 76)

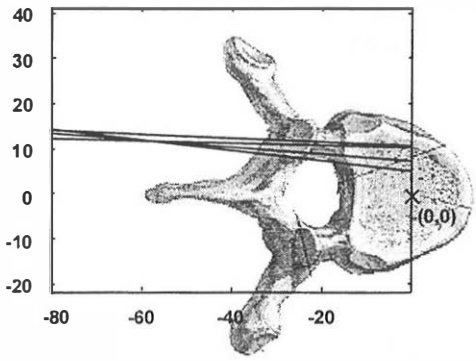

Fig. 15 - Axes of rotation during the second compression (lower part of the sternum)

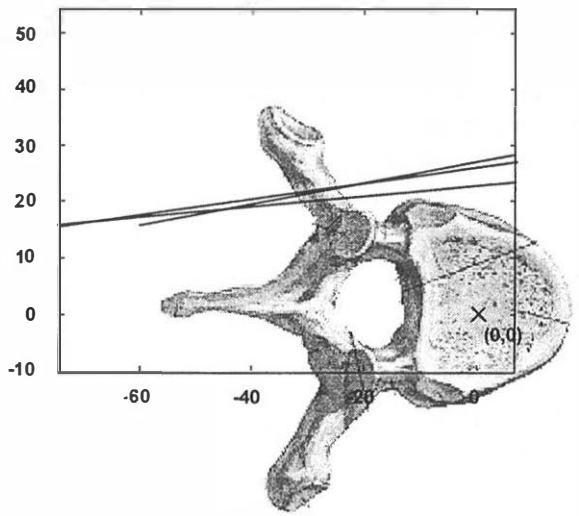

Fig. 16 - Axes of rotation during the third compression (upper part of the sternum)

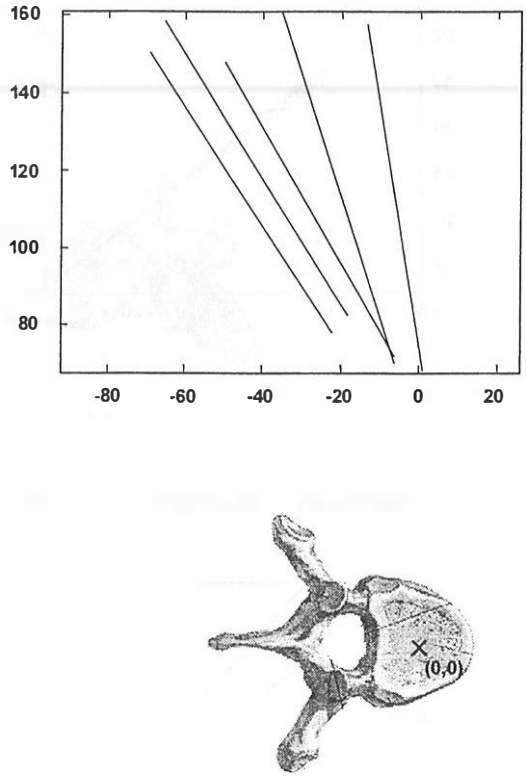

Fig. 17 - Axes of rotation during the compression without intercostal muscles (middle of the sternum)

Side views of these same axes are represented on figures 19 to 22.

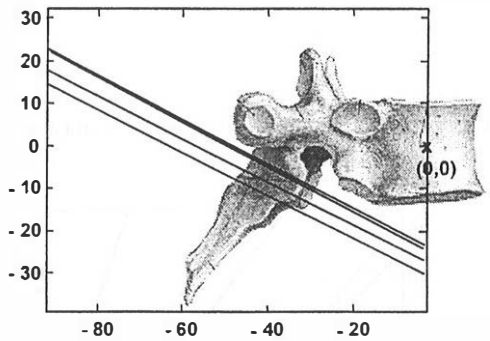

Fig. 18 - Axes of rotation during the first compression (middle of the sternum)

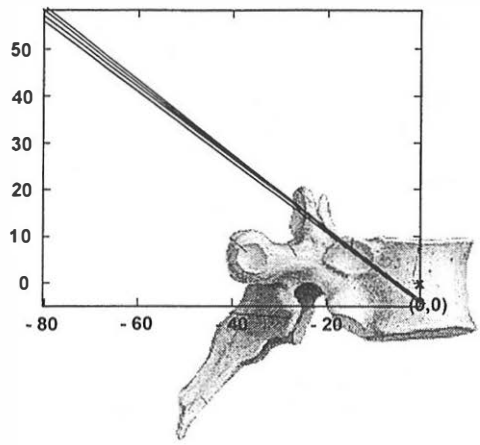

Fig. 19 - Axes of rotation during the second compression (lower part of the sternum)

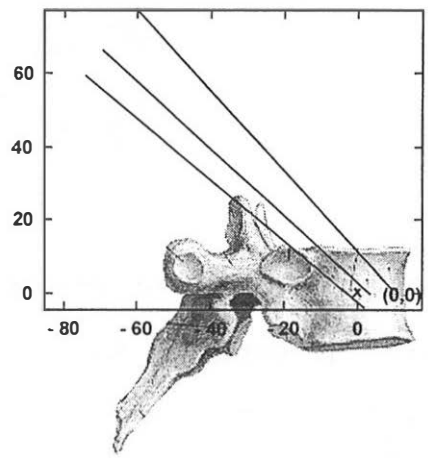

Fig. 20 - Axes of rotation during the third compression (upper part of the sternum)

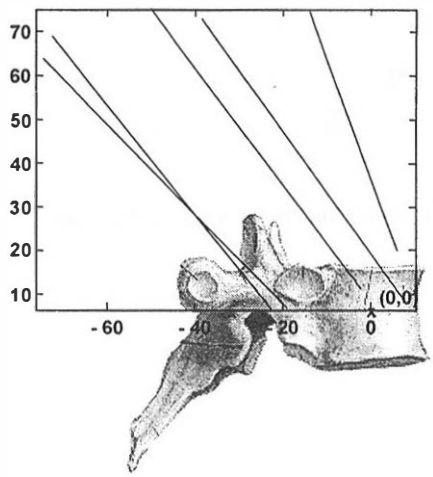

Fig. 21 - Axes of rotation during the compression without intercostal muscles (middle of the sternum)

DISCUSSION AND CONCLUSION

The small amplitude of the marker displacements and the relative importance of the measurement noise does not allow for an accurate monitoring of the displacements of the rotation axis. But thanks to solidification technique and averaging on several pictures, several axes of rotation of the ribs with respect to their corresponding vertebrae have been calculated during frontal compressions of the thoracic cage.

The result show that, for a given application point, with intercostal muscles, the orientation of the rotation axis remain relatively constant. The calculated axis of rotation seems to migrate slightly during compression (see Fig. 14 to Fig. 16 and Fig. 18 to Fig. 20) while remaining parallel to a fixed direction. The axis is roughly directed outward and rearward. But the orientation of the axes changes with the point where the force is applied.

The amplitude of the rib rotation depends on the location of force application. When the compression force is applied in the middle of the sternum, with intercostal muscles, the maximum of rib rotation is obtained for the 3rd rib and is less than 10 degrees. When the compression force is applied in the lower part of the sternum, the maximum amplitude of rotation is 17 degrees (maximum obtained for the 5th rib). Finally, when the compression is applied in the upper part of the sternum, the amplitude of rotation is less than 6 degrees (maximum obtained for the 3rd rib).

For each compression, the amplitude of rotation of the 7th rib is less than 3 degrees with intercostal muscles. As a result, the axis of rotation of the 7th rib has not been determined. The behaviour of the 3rd rib is quite similar to that of the 5th rib with difference in axis orientation.

These results show that the hypothesis of a fixed axis of rotation in the movement between ribs and vertebrae, described by Kapandji for breathing movements, is not valid in this loading context.

When the intercostal muscles are taken away, the axes are much more scattered. Therefore, the intercostal muscles contribute to maintain the cohesion of the thoracic cage.

If these results are confirmed, the costovertebral articulation will not be considered as a kinematic joint and will not be represented by a fixed axis pivot in the model of the thoracic cage. Instead a stiffness matrix will have to be identified in order to model the costo-vertebral connection by a general 3D spring. The coefficients if this matrix will be identified from our experimental data and measurements of the stiffness of this articulation described in other studies (Descrimes, 1995), (Lemosse, 1998).

The data of the two other triplets located near the chondro-costal joint and near the middle of the rib have not been analysed until now. They will be analyzed later on and will give information on the amount of deformation of the ribs and on the influence of the intercostal muscles on the stability of the rib cage.

Subsquently, we intend to use these results to improve the simulation of global deformation of the model of the thoracic cage when different forces are applied on the sternum.

ACKNOWLEDGEMENTS

This research is carried out in co-operation with the Accidentology and Biomechanics Laboratory of Peugeot-Citroën and Renault (LAB) and is partially supported by the French Ministry of Industry.

Thanks to P. Lapelerie, X. Michel, M. Ramet, A. Gilibert, J. Lardière, A. Maupas and all the LBMC team for their precious help in this work.

ANNEX

DESCRIPTION OF THE TECHNIQUE USED TO DETERMINE THE AXES OF ROTATION

For each rib, the triplet located near the costovertebral joint provide a local reference frame. The matrix of rotation between the position of this frame at each step of compression (every 5 mm) and the position of it initially (without loading) is determined.

$$R = \begin{pmatrix} a11 & a12 & a13 \\ a21 & a22 & a23 \\ a31 & a32 & a33 \end{pmatrix}$$

According to the method of Rodrigues, the coordinates (k_1, k_2, k_3) of the directing vector of the axis of rotation $\vec{k}$ (in the reference frame of the triplet in the initial position) and the angle of rotation around this axis θ are determined at each step of compression.

$$\theta = Arccos\left(\frac{a11 + a22 + a33 - 1}{2}\right)$$

$$k_1 = \frac{a32 - a23}{2\sin\theta} \qquad k_2 = \frac{a13 - a31}{2\sin\theta} \qquad k_3 = \frac{a21 - a12}{2\sin\theta}$$

The position of the reference frame attached to the triplet in the initial position with respect to the rig reference frame is known during compression. The coordinates (k_1, k_2, k_3) are then calculated in the anatomic reference frame of the corresponding vertebrae thanks to the transformation matrix between rig and anatomical reference frames which is the product of the transformation matrix between technical and anatomical reference frames and the one between rig and technical references frames.

All the axes obtained at each step of compression are at least represented in a graphics with the corresponding vertebrae.

REFERENCES

Kapandji I.A. (1994) Physiologie Articulaire. Tronc et rachis. 5ème édition. Maloine, Paris.

Allain J.C., Trameçon A., Pormenté S. (1998) Etude et calibration d'un modèle numérique de thorax. Rapport confidentiel. E.S.I Group, Rungis, France(94).

Chèze L. Fregly B.J., Dimnet J. (1995) A solidification procedure to facilitate kinematic analyses based on video system data. Journal of Biomechanics, vol.28, n°7, 879-884.

Descrimes J.L. (1995) Modélisation biomécanique par éléments finis du rachis et de la cage thoracique pour l'étude des déformations scoliotiques. Thèse de Mécanique. ENSAM, Paris.

Faro Arm (1997) © Faro Technologies Inc.

Lemosse D., Le Rue O., Diop A., Skalli W., Marec P., Lavaste F. (1998) Characterization of the mechanical behaviour of the costovertebral joint. Eur. Spine J. 7:16-23. © Springer-Verlag.

N.T.C Limited (1994) News Technologies Corp. LTD, Logiciel 3D Vision version 3.0 © D. Dietrich.

Reddi M.M., TSAI H.C. (1977) Computer Simulation of Human Thoracic Skeletal Response. Final Report Contract (vol. 1 and 2) DOT HS 803209. U.S Department of Transportation NHTSA, Washington D.C., USA.

Roberts S.B. (1979) Simulation of Thoracic Impact Experiments using Thorax V Computer Model. Final Report. Contract DOT-NHTSA. 9-6577, September 1979.

Rodrigues O. (1840) Des lois géométriques qui régissent les déplacements d'un système solide dans l'espace et de la variation des coordonnées provenant de ces déplacements considérés indépendamment des causes qui peuvent les produire. Journal Math. Pures Appli, 5, 380-440.

Rohen J.W., Yokochi C., Lütjen-Drecoll E. (1999) Anatomie Humaine. 3ème édition. Atlas photographique d'Anatomie systématique et topographique. Maloine, Paris.

Song E., Lizee E., Robin S., Bertholon N., Lavaste F. (1998) Development of a finite element model of the human body. 42nd Annual Stapp Car Crash Conference, p337. Tempa, Arizona, USA.

Sundaram S.H., Feng C.C. (1977) Finite Element Analysis of the Human Thorax. J. Of Biomechanics, 10, pp 505-516.